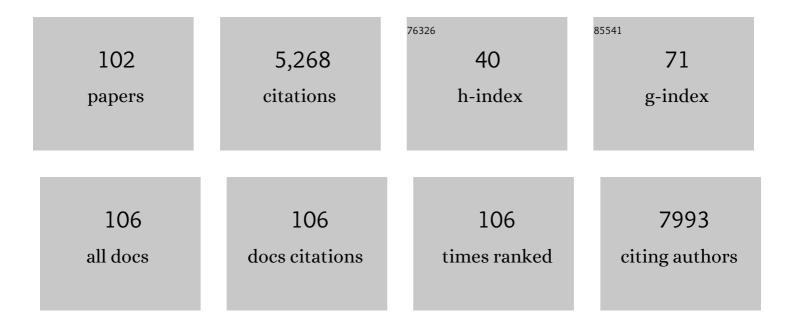
List of Publications by Year in descending order

Source: https://exaly.com/author-pdf/2704265/publications.pdf Version: 2024-02-01



#	Article	IF	CITATIONS
1	Nanocrystalline triple perovskite compounds A ₃ Fe ₂ BO ₉ (A = Sr,) Tj ETQq1 Materials Chemistry Frontiers, 2022, 6, 1116-1128.	1 0.78431 5.9	.4 rgBT /C∨ 11
2	Bandgap Engineering in Novel Fluoriteâ€Type Rare Earth Highâ€Entropy Oxides (REâ€HEOs) with Computational and Experimental Validation for Photocatalytic Water Splitting Applications. Advanced Sustainable Systems, 2022, 6, .	5.3	22
3	Synthesis of Ti(OH)OF â< 0.66 H 2 O in Imidazoliumâ€based Ionic Liquids. ChemistryOpen, 2021, 10, 1	811.9188.	1
4	Single crystal growth, structural characterization and magnetic properties study of an antiferromagnetic trinuclear iron(III) acetate complex with uncoordinated hexamine. Inorganica Chimica Acta, 2021, 520, 120292.	2.4	6
5	Triple perovskite-based triboelectric nanogenerator: a facile method of energy harvesting and self-powered information generator. Materials Today Energy, 2021, 20, 100639.	4.7	28
6	Sol-Gel Synthesis of Ceria-Zirconia-Based High-Entropy Oxides as High-Promotion Catalysts for the Synthesis of 1,2-Diketones from Aldehyde. Molecules, 2021, 26, 6115.	3.8	9
7	Ionic liquid-mediated low-temperature formation of hexagonal titanium-oxyhydroxyfluoride particles. CrystEngComm, 2020, 22, 1568-1576.	2.6	2
8	sReactivation of CeO 2 â€based Catalysts in the HCl Oxidation Reaction: In situ Quantification of the Degree of Chlorination and Kinetic Modeling. ChemCatChem, 2020, 12, 5511-5522.	3.7	8
9	Impact of Aliovalent/Isovalent Ions (Gd, Zr, Pr, and Tb) on the Catalytic Stability of Mesoporous Ceria in the HCl Oxidation Reaction. ACS Applied Nano Materials, 2020, 3, 7406-7419.	5.0	9
10	Mixed Ru <i>_x</i> lr _{1–<i>x</i>} O ₂ Oxide Catalyst with Well-Defined and Varying Composition Applied to CO Oxidation. Journal of Physical Chemistry C, 2020, 124, 18670-18683.	3.1	17
11	Nanocrystalline Antiferromagnetic High- \hat{I}^{2} Dielectric Sr2NiMO6 (M = Te, W) with Double Perovskite Structure Type. Molecules, 2020, 25, 3996.	3.8	23
12	Rational Sol–Gel-Based Synthesis Design and Magnetic, Dielectric, and Optical Properties Study of Nanocrystalline Sr ₃ Co ₂ WO ₉ Triple Perovskite. Journal of Physical Chemistry C, 2020, 124, 12794-12807.	3.1	19
13	Size reduction-induced properties modifications of antiferromagnetic dielectric nanocrystalline Ba2NiMO6 (M = W, Te) double perovskites. Oxford Open Materials Science, 2020, 1, .	1.8	2
14	CeO ₂ Wetting Layer on ZrO ₂ Particle with Sharp Solid Interface as Highly Active and Stable Catalyst for HCl Oxidation Reaction. ACS Catalysis, 2019, 9, 10680-10693.	11.2	20
15	Efficient and Stable FASnI ₃ Perovskite Solar Cells with Effective Interface Modulation by Lowâ€Dimensional Perovskite Layer. ChemSusChem, 2019, 12, 5007-5014.	6.8	111
16	Structural characterization and magnetic property determination of nanocrystalline Ba ₃ Fe ₂ WO ₉ and Sr ₃ Fe ₂ WO ₉ perovskites prepared by a modified aqueous sol–gel route. CrystEngComm, 2019, 21, 218-227.	2.6	12
17	Oxygen storage capacity <i>versus</i> catalytic activity of ceria–zirconia solid solutions in CO and HCl oxidation. Catalysis Science and Technology, 2019, 9, 2163-2172.	4.1	37
18	The stabilizing effect of water and high reaction temperatures on the CeO2-catalyst in the harsh HCl oxidation reaction, Journal of Catalysis, 2018, 357, 257-262.	6.2	18

#	Article	IF	CITATIONS
19	Catalytic HCl oxidation reaction: Stabilizing effect of Zr-doping on CeO2 nano-rods. Applied Catalysis B: Environmental, 2018, 239, 628-635.	20.2	34
20	Sustainable and surfactant-free high-throughput synthesis of highly dispersible zirconia nanocrystals. Journal of Materials Chemistry A, 2017, 5, 16296-16306.	10.3	8
21	In Situ Study of the Oxygen-Induced Transformation of Pyrochlore Ce ₂ Zr ₂ O _{7+<i>x</i>} to the κ-Ce ₂ Zr ₂ O ₈ Phase. Chemistry of Materials, 2017, 29, 9218-9226.	6.7	20
22	Graphene-oxide-wrapped ZnMn ₂ O ₄ as a high performance lithium-ion battery anode. Nanotechnology, 2017, 28, 455401.	2.6	17
23	Shape-Controlled CeO ₂ Nanoparticles: Stability and Activity in the Catalyzed HCl Oxidation Reaction. ACS Catalysis, 2017, 7, 6453-6463.	11.2	109
24	Synthesis and full characterization of the phase-pure pyrochlore Ce2Zr2O7 and the κ-Ce2Zr2O8 phases. Applied Catalysis B: Environmental, 2016, 197, 23-34.	20.2	28
25	Combustion synthesized hierarchically porous WO3 for selective acetone sensing. Materials Chemistry and Physics, 2016, 184, 155-161.	4.0	25
26	Aqueous Sol–Gel Route toward Selected Quaternary Metal Oxides with Single and Double Perovskite-Type Structure Containing Tellurium. Crystal Growth and Design, 2016, 16, 2535-2541.	3.0	12
27	Facile synthesis of CuO micro-sheets over Cu foil in oxalic acid solution and their sensing properties towards n-butanol. Journal of Materials Chemistry C, 2016, 4, 985-990.	5.5	14
28	Controllable synthesis and change of emission color from green to orange of ZnO quantum dots using different solvents. New Journal of Chemistry, 2015, 39, 2881-2888.	2.8	50
29	Long cycle life of CoMn ₂ O ₄ lithium ion battery anodes with high crystallinity. Journal of Materials Chemistry A, 2015, 3, 14759-14767.	10.3	72
30	Ionic liquid- and surfactant-controlled crystallization of WO ₃ films. Physical Chemistry Chemical Physics, 2015, 17, 18138-18145.	2.8	13
31	A high-performance n-butanol gas sensor based on ZnO nanoparticles synthesized by a low-temperature solvothermal route. RSC Advances, 2015, 5, 54372-54378.	3.6	74
32	Hydrothermal synthesis of single crystal CoAs ₂ O ₄ and NiAs ₂ O ₄ compounds and their magnetic properties. RSC Advances, 2015, 5, 18280-18287.	3.6	9
33	Nanoparticle cluster gas sensor: Pt activated SnO ₂ nanoparticles for NH ₃ detection with ultrahigh sensitivity. Nanoscale, 2015, 7, 14872-14880.	5.6	284
34	Two-Dimensional Atomic Crystals: Paving New Ways for Nanoelectronics. Journal of Electronic Materials, 2015, 44, 4080-4097.	2.2	6
35	NiO nanosheets assembled into hollow microspheres for highly sensitive and fast-responding VOC sensors. RSC Advances, 2015, 5, 80786-80792.	3.6	14
36	Enhancing phosphate removal from water by using ordered mesoporous silica loaded with samarium oxide. Analytical Methods, 2015, 7, 10052-10060.	2.7	17

#	Article	IF	CITATIONS
37	Porous NiO nanosheets self-grown on alumina tube using a novel flash synthesis and their gas sensing properties. RSC Advances, 2015, 5, 4880-4885.	3.6	52
38	Combustion synthesis of porous Pt-functionalized SnO ₂ sheets for isopropanol gas detection with a significant enhancement in response. Journal of Materials Chemistry A, 2014, 2, 20089-20095.	10.3	106
39	Chromium coordination compounds with bis(3,5-dimethylpyrazol-1-yl)acetic acid or its anion. Polyhedron, 2014, 70, 119-124.	2.2	2
40	Large-Pore Mesoporous Ho3Fe5O12 Thin Films with a Strong Room-Temperature Perpendicular Magnetic Anisotropy by Sol–Gel Processing. Chemistry of Materials, 2014, 26, 2337-2343.	6.7	13
41	Novel Mixed Phase SnO ₂ Nanorods Assembled with SnO ₂ Nanocrystals for Enhancing Gas-Sensing Performance toward Isopropanol Gas. Journal of Physical Chemistry C, 2014, 118, 9832-9840.	3.1	146
42	Hydrothermal growth of ZnO nanorods on Zn substrates and their application in degradation of azo dyes under ambient conditions. CrystEngComm, 2014, 16, 7761-7770.	2.6	42
43	Photocatalytic degradation properties of Ni(OH)2 nanosheets/ZnO nanorods composites for azo dyes under visible-light irradiation. Ceramics International, 2014, 40, 57-65.	4.8	62
44	Morphology, Microstructure, and Magnetic Properties of Ordered Large-Pore Mesoporous Cadmium Ferrite Thin Film Spin Glasses. Inorganic Chemistry, 2013, 52, 3744-3754.	4.0	38
45	A facial method to synthesize Ni(OH)2 nanosheets for improving the adsorption properties of Congo red in aqueous solution. Powder Technology, 2013, 235, 121-125.	4.2	23
46	Functionalization of plasmonic metamaterials utilizing metal–organic framework thin films. Physica Scripta, 2012, T149, 014051.	2.5	3
47	Surfactant-assisted synthesis of CeO2 nanoparticles and their application in wastewater treatment. RSC Advances, 2012, 2, 12413.	3.6	186
48	Soft-templating synthesis of mesoporous magnetic CuFe2O4 thin films with ordered 3D honeycomb structure and partially inverted nanocrystalline spinel domains. Chemical Communications, 2012, 48, 4471.	4.1	81
49	Structural analysis of monolayered and bilayered SnO2 thin films. Surface and Coatings Technology, 2012, 211, 24-28.	4.8	4
50	Nanocrystalline NiMoO4 with an ordered mesoporous morphology as potential material for rechargeable thin film lithium batteries. Chemical Communications, 2012, 48, 6726.	4.1	125
51	Nanocrystalline hybrid inorganic–organic one-dimensional chain systems tailored with 2- and 3-phenyl ring monocarboxylic acids. Journal of Materials Chemistry, 2012, 22, 10255.	6.7	5
52	Mesoporous MgTa ₂ O ₆ thin films with enhanced photocatalytic activity: On the interplay between crystallinity and mesostructure. Beilstein Journal of Nanotechnology, 2012, 3, 123-133.	2.8	9
53	Interplay between the structural and magnetic probes in the elucidation of the structure of a novel 2D layered [V4O4(OH)2(O2CC6H4CO2)4]·DMF. Dalton Transactions, 2012, 41, 581-589.	3.3	8
54	Structural analysis of amorphous-nanocrystalline silicon thin films by grazing incidence X-ray diffraction. Nuclear Instruments & Methods in Physics Research B, 2012, 284, 78-82.	1.4	9

IGOR DJERDJ

#	Article	IF	CITATIONS
55	Microwave-Assisted Nonaqueous Solâ^'Gel Chemistry for Highly Concentrated ZnO-Based Magnetic Semiconductor Nanocrystals. Journal of Physical Chemistry C, 2011, 115, 1484-1495.	3.1	111
56	Ionicâ€Liquid Synthesis Route of TiO ₂ (B) Nanoparticles for Functionalized Materials. Chemistry - A European Journal, 2011, 17, 775-779.	3.3	65
57	The double role of p-toluenesulfonic acid in the formation of ZnO particles with different morphologies. CrystEngComm, 2010, 12, 1862.	2.6	19
58	Co-Doped ZnO nanoparticles: Minireview. Nanoscale, 2010, 2, 1096.	5.6	124
59	Solvothermal and surfactant-free synthesis of crystalline Nb2O5, Ta2O5, HfO2, and Co-doped HfO2 nanoparticles. Physical Chemistry Chemical Physics, 2010, 12, 15537.	2.8	61
60	Toward a Low-Temperature Solâ^'Gel Synthesis of TiO ₂ (B) Using Mixtures of Surfactants and Ionic Liquids. Chemistry of Materials, 2010, 22, 3502-3510.	6.7	56
61	Niobium Doped TiO ₂ with Mesoporosity and Its Application for Lithium Insertion. Chemistry of Materials, 2010, 22, 6624-6631.	6.7	127
62	Structural Characterization of a Nanocrystalline Inorganicâ ^{°°} Organic Hybrid with Fiberlike Morphology and One-Dimensional Antiferromagnetic Properties. Chemistry of Materials, 2009, 21, 3356-3369.	6.7	36
63	Structure and electrical conductivity of porous zirconium titanate ceramics produced by mechanochemical treatment and sintering. Journal of Alloys and Compounds, 2009, 479, 525-531.	5.5	26
64	Antimony-Doped SnO ₂ Nanopowders with High Crystallinity for Lithium-Ion Battery Electrode. Chemistry of Materials, 2009, 21, 3202-3209.	6.7	172
65	Neodymium Dioxide Carbonate as a Sensing Layer for Chemoresistive CO ₂ Sensing. Chemistry of Materials, 2009, 21, 5375-5381.	6.7	88
66	Layered hybrid organic–inorganic nanobelts exhibiting a field-induced magnetic transition. Physical Chemistry Chemical Physics, 2009, 11, 6166.	2.8	25
67	Efficient microwave-assisted synthesis of LiFePO4 mesocrystals with high cycling stability. Journal of Materials Chemistry, 2009, 19, 5125.	6.7	80
68	Correlation Between the Microstructure and the Electrical Properties of ZrTiO ₄ Ceramics. Journal of the American Ceramic Society, 2008, 91, 178-186.	3.8	18
69	Polymerâ€Assisted Generation of Antimonyâ€Đoped SnO ₂ Nanoparticles with High Crystallinity for Application in Gas Sensors. Small, 2008, 4, 1656-1660.	10.0	121
70	Nonaqueous synthesis of metal oxide nanoparticles: Short review and doped titanium dioxide as case study for the preparation of transition metal-doped oxide nanoparticles. Journal of Solid State Chemistry, 2008, 181, 1571-1581.	2.9	94
71	Nanostructure of thin silicon films by combining HRTEM, XRD and Raman spectroscopy measurements and the implication to the optical properties. Applied Surface Science, 2008, 254, 2748-2754.	6.1	32
72	Generalized Nonaqueous Sol–Gel Synthesis of Different Transitionâ€Metal Niobate Nanocrystals and Analysis of the Growth Mechanism. Chemistry - an Asian Journal, 2008, 3, 746-752.	3.3	37

#	Article	IF	CITATIONS
73	Diluted magnetic semiconductors: Mn/Co-doped ZnO nanorods as case study. Journal of Materials Chemistry, 2008, 18, 5208.	6.7	112
74	One-minute synthesis of crystalline binary and ternary metal oxide nanoparticles. Chemical Communications, 2008, , 886-888.	4.1	295
75	Influence of mechanochemical processing to luminescence properties in Y2O3 powder. Journal of Alloys and Compounds, 2008, 456, 313-319.	5.5	54
76	IL-assisted synthesis of V2O5 nanocomposites and VO2 nanosheets. Journal of Materials Chemistry, 2008, 18, 5761.	6.7	38
77	Oxygen Self-Doping in Hollandite-Type Vanadium Oxyhydroxide Nanorods. Journal of the American Chemical Society, 2008, 130, 11364-11375.	13.7	39
78	Implantation conditions for diamond nanocrystal formation in amorphous silica. Journal of Applied Physics, 2008, 104, 034315.	2.5	2
79	Metal Oxide Nanocrystals: Building Blocks for Mesostructures and Precursors for Metal Nitrides. Materials Research Society Symposia Proceedings, 2007, 1007, 1.	0.1	0
80	Nonaqueous Synthesis of Colloidal ZnGa2O4Nanocrystals and Their Photoluminescence Properties. Chemistry of Materials, 2007, 19, 5830-5832.	6.7	45
81	Nonaqueous Synthesis of Nanocrystalline Indium Oxide and Zinc Oxide in the Oxygen-Free Solvent Acetonitrile. Crystal Growth and Design, 2007, 7, 113-116.	3.0	60
82	Nonaqueous Synthesis of Manganese Oxide Nanoparticles, Structural Characterization, and Magnetic Properties. Journal of Physical Chemistry C, 2007, 111, 3614-3623.	3.1	120
83	Thermal Transformation of Metal Oxide Nanoparticles into Nanocrystalline Metal Nitrides Using Cyanamide and Urea as Nitrogen Source. Chemistry of Materials, 2007, 19, 3499-3505.	6.7	115
84	Nonaqueous Sol–Gel Synthesis of a Nanocrystalline InNbO ₄ Visible‣ight Photocatalyst. Advanced Materials, 2007, 19, 2083-2086.	21.0	123
85	Low wavenumber Raman scattering of nanoparticles and nanocomposite materials. Journal of Raman Spectroscopy, 2007, 38, 647-659.	2.5	73
86	The influence of post deposition plasma treatment on SnOx structural properties. Vacuum, 2007, 82, 266-269.	3.5	2
87	The influence of local structure of nanocrystalline Ni films on the catalytic activityâ~†. Electrochemistry Communications, 2007, 9, 299-302.	4.7	11
88	Structural study of nanocrystalline nickel thin films. Journal of Applied Crystallography, 2007, 40, s377-s382.	4.5	7
89	Direct Lowâ€Temperature Synthesis of Rutile Nanostructures in Ionic Liquids. Small, 2007, 3, 1753-1763.	10.0	169
90	Morphology-controlled nonaqueous synthesis of anisotropic lanthanum hydroxide nanoparticles. Journal of Solid State Chemistry, 2007, 180, 2154-2165.	2.9	76

#	Article	IF	CITATIONS
91	Nonaqueous Synthesis of Uniform Indium Tin Oxide Nanocrystals and Their Electrical Conductivity in Dependence of the Tin Oxide Concentration. Chemistry of Materials, 2006, 18, 2848-2854.	6.7	157
92	Structural investigations of nanocrystalline TiO2 samples. Journal of Alloys and Compounds, 2006, 413, 159-174.	5.5	165
93	Mechanism of ZrTiO4 Synthesis by Mechanochemical Processing of TiO2 and ZrO2. Journal of the American Ceramic Society, 2006, 89, 060427083300025-???.	3.8	20
94	Transmission electron microscopy study of carbon nanophases produced by ion beam implantation. Materials Science and Engineering C, 2006, 26, 1202-1206.	7.3	6
95	Preparation of a large Mesoporous CeO2 with crystalline walls using PMMA colloidal crystal templates. Colloid and Polymer Science, 2006, 285, 1-9.	2.1	48
96	Preparation of nanostructured ZrTiO4 by solid state reaction in equimolar mixture of TiO2 and ZrO2. Crystal Research and Technology, 2006, 41, 1076-1081.	1.3	21
97	Structural Refinement of Nanocrystalline TiO2 Samples. , 2006, , 497-501.		2
98	Transmission electron microscopy studies of nanostructured TiO2 films on various substrates. Vacuum, 2005, 80, 371-378.	3.5	23
99	XRD line profile analysis of tungsten thin films. Vacuum, 2005, 80, 151-158.	3.5	30
100	Determination of Nanosize Particle Distribution by Low Frequency Raman Scattering: Comparison to Electron Microscopy. Lecture Notes in Physics, 2002, , 24-36.	0.7	4
101	An analysis of evolution of grain size-lattice parameters dependence in nanocrystalline TiO2 anatase. Materials Science and Engineering C, 2002, 19, 85-89.	7.3	49
102	Evidence from HRTEM image processing, XRD and EDS on nanocrystalline iron-doped titanium oxide powders. Materials Science and Engineering B: Solid-State Materials for Advanced Technology, 2001, 85, 55-63.	3.5	34